Journal of Physics: Conference Series **668** (2016) 012002 doi:10.1088/1742-6596/668/1/012002

Freeze-out, Hadronization and Statistical Model

Paolo Castorina

Dipartimento di Fisica ed Astronomia, Universita' di Catania and INFN Sezione di Catania, Italy

E-mail: paolo.castorina@ct.infn.it

Abstract. The comparison of the statistical hadronization model with experimental data and lattice QCD results is not always straightforward. Indeed, the interpretation of the ϕ meson production, of the proton to pion multiplicity ratio at LHC and the agreement of the freeze-out curve with the lattice critical line in the $T-\mu_B$ plane, require further analyses. Moreover the dynamics of the hadronization has to be compatible with: 1) the statitical behavior also observed in elementary high energy collisions; 2) a universal hadronization temperature for all high energy collisions; 3) the freeze-out criteria. In these lecture notes the SHM is recalled and some explanations of the puzzling aspects of its comparison with data are discussed.

1. Introduction

The statistical hadronization model (SHM) [1, 2, 3, 4, 5] is a useful tool to describe the hadron formation at a scale where QCD is no longer perturbative and it has to be interpreted as a coarse grained approach which, with a small number of parameters, successfully describes the experimental data of the particle yields, of the low transverse momentum spectra and gives the dependence on the baryochemical potential, μ_B, of the chemical freeze-out temperature, T_{ch}, i.e. the temperature where subsequent inelastic collisions between hadrons cease.

However, the comparison of the SHM with experimental and lattice results is not always straightforward and, for example, the interpretation of the ϕ meson production, of the proton to pion multiplicity ratio at LHC and the comparison of the freeze-out curve with the lattice critical line in the $T-\mu_B$ plane [6, 7] require further analyses. In these lecture notes the SHM and, in particular, some puzzling aspects of its comparison with data are reviewed.

In Sec. 2 the SHM is briefly summarized and Sec. 3 contains its comparison with specific experimental data and lattice results which opens interesting questions on the underlying dynamics. Sec.4 discusses the possible answers to the previous questions within the SHM or by introducing some modifications, completely consistent with the statistical approach. A possible understanding of other puzzling aspects, concerning the application of the SHM to elementary (e^+e^- and hadron-hadron) collisions, the universality of the freeze-out temperature in all high energy collisions and the theoretical basis of the freeze-out criteria, are recalled in Sec. 5, where hadronization is interpreted as the Hawking-Unruh radiation in QCD. Comments and conclusions are given in Sec. 6.

2. Statistical hadronization model

The statistical hadronization model assumes that hadronization in high energy collisions is a universal process proceeding through the formation of multiple colorless massive clusters (or

fireballs) of finite spatial extension. These clusters are taken to decay into hadrons according to a purely statistical law: every multi-hadron state of the cluster phase space defined by its mass, volume and charges is equally probable. The mass distribution and the distribution of charges (electric, baryonic and strange) among the clusters and their (fluctuating) number are determined in the prior dynamical stage of the process. Once these distributions are known, each cluster can be hadronized on the basis of statistical equilibrium, leading to the calculation of averages in the *microcanonical ensemble*, enforcing the exact conservation of energy and charges of each cluster.

Hence, in principle, one would need the mentioned dynamical information in order to make definite quantitative predictions to be compared with data. Nevertheless, for Lorentz-invariant quantities such as multiplicities, one can introduce a simplifying assumption and thereby obtain a simple analytical expression in terms of a temperature. The key point is to assume that the distribution of masses and charges among clusters is again purely statistical [5]. Therefore, as far as the calculation of multiplicities is concerned, the set of clusters becomes equivalent, on average, to a large cluster (*equivalent global cluster*) whose volume is the sum of proper cluster volumina and whose charge is the sum of cluster charges (and thus the conserved charge of the initial colliding system). In such a global averaging process, the equivalent cluster generally turns out to be large enough in mass and volume so that the canonical ensemble becomes a good approximation. In other words, a temperature can be introduced which replaces the *a priori* more fundamental description in terms of an energy density.

To obtain a simple expression for our further discussion, we neglect for the moment an aspect which is important in any actual analysis. Although in elementary collisions the conservation of the various discrete Abelian charges (electric charge, baryon number, strangeness, heavy flavour) has to be taken into account *exactly* [8, 9], as we shall discuss in detail in Sec. 4, we here consider for the moment a grand canonical picture. In general the average multiplicity of a given hadronic species i then becomes

$$\langle n_i \rangle^{\text{primary}} = d_i \frac{VT}{(2\pi)^3} \int d^3p \frac{1}{\gamma_s^{-s_i} \exp[(E_i - \vec{\mu}\vec{q}_i)/T_{ch}] \pm 1}, \tag{1}$$

where d_i is the degeneracy factor, $E_i = \sqrt{p^2 + m_i^2}$ is the particle energy, s_i is the number of strange quarks/antiquarks it contains, $\vec{\mu}_i$ are the chemical potentials associated with the conserved charges $\vec{q}_i$, V denotes the overall equivalent cluster volume, γ_s is the parameter describing the strangeness suppression.

Here primary indicates that it gives the average number at the hadronization point, prior to all subsequent resonance decays. As a second step, all resonances in the gas which are unstable against strong decays are allowed to decay in lighter stable hadrons, using appropriate branching ratios for the decay published by the Particle Data Group [10].

A typical fit of the experimental data in the SHM contains four parameters: T_{ch}, V, μ_B and γ_s and the strangeness suppression implies $\gamma_s < 1$ in elementary collisions.

In conclusion, the dynamics of the SHM corresponds to a gas of free hadronic resonances (HRG) at fixed temperature and chemical potentials which includes the known resonances up to a large mass (in general $2 - 2.5$ GeV).

In the next section we shall discuss some aspects of the comparison of the SHM with data.

3. Statistical hadronization model versus experimental data

Intuitively one expects a statistical behavior when there is a large number of partons in the initial state and/or of hadrons in the final state, but an interesting aspect of the SHM is that it is in good agreement with data for elementary collisions also [3, 4].

For example, the comparison of the SHM fit to the p+p data for the abundances of about 20 different species for collisions at $\sqrt{s} = 200$ GeV, reported in table 1 of Ref. [11], gives a χ^2/ d.o.f. $= 15.6/14$, with $\gamma_s \simeq 0.6$ and $T_{ch} \simeq 170$ MeV. Surprising enough, also for e^+e^- there is a good agreement with data, although the implementation of the SHM, the effective meaning of the χ^2/d.o.f and the role of heavy quarks produced in the initial state by the virtual photon need some specifications [11, 12, 13, 14].

The strangeness suppression in elementary collisions is reported in Fig. 1 [15] and the enhancement in nucleus-nucleus scattering [16] is depicted in Fig. 2 ($\gamma_s \to 1$) [15].

The compilation of the freeze-out temperatures for high energy ($\sqrt{s} \geq 20$ GeV) elementary and nucleus-nucleus collisions up to RHIC energy is reported in Fig. 3 and the independence of the hadronization temperature on the initial setting of the scattering (elementary particles or nuclei) clearly calls for a universal temperature for all high energy collisions.

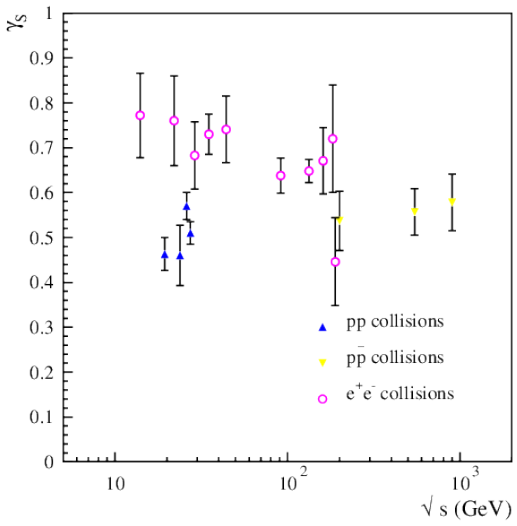

Figure 1. Strangeness suppression, i.e. $\gamma_s < 1$, in elementary collisions, from Ref. [15].

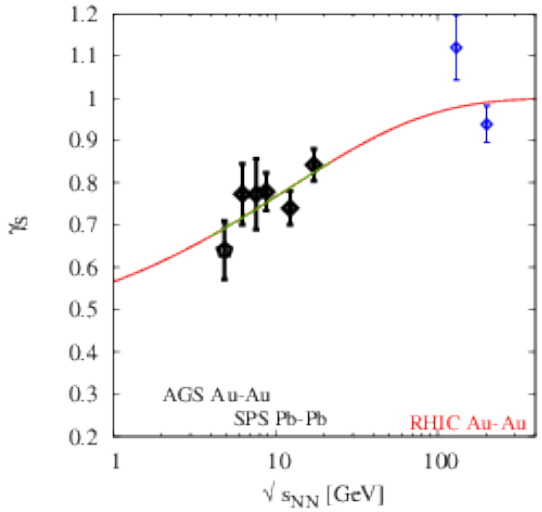

Figure 2. Strangeness enhancement in heavy ion collisions, i.e. $\gamma_s \to 1$, in the grand canonical description, Eq. (2). From Ref. [15].

The fits to the relativistic heavy ion data require the further parameter μ_B, describing the baryon density, which turns out to be directly correlatd with the collision energy. The baryon-chemical potential sharply decreases with increasing energy (μ_B is only a few MeV at RHIC energy and $\mu_B \simeq 0$ at LHC). The freeze-out temperature strongly depends on $\sqrt{s}$ at low energy, i.e. on the baryon density at large μ_B, and one obtains the freeze-out curve in fig.4 where is also reported the result of the recent fit to LHC ALICE data [17] (see later) and depicted are the curves obtained by imposing specific, intriguing, criteria. Indeed, the phenomenological freeze-out curve can be described by requiring that the average energy per particle , $< E > / < N >$ is about 1.08 GeV and/or that the ratio between the entropy density, s and T^3_{ch} is about 7 [18, 19, 20, 21, 22, 23, 24]. The latter result is completely consistent with lattice data on s/T^3 at the critical temperature, for $\mu_B = 0$ [25].

Finally, the recent LHC data are in good agreement with the SHM, however the proton to pion multiplicity ratio shows a discrepancy of about 3 standard deviations (see Fig. 6) [26, 27].

The previous brief summary of the comparison of the SHM with data calls for an understanding of the hadronization process which answers the following questions:

- Why is strangeness production universally suppressed in elementary collisions?

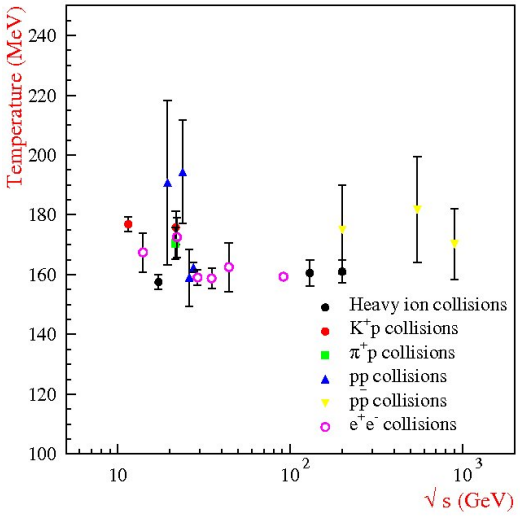

Figure 3. Universal behavior of freeze-out temperature for elementary and heavy ion collisions at high energy.

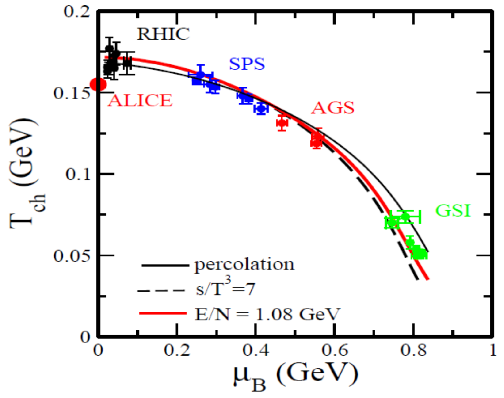

Figure 4. Freeze-out curve from SHM and comparison with the freeze-out criteria, see text.

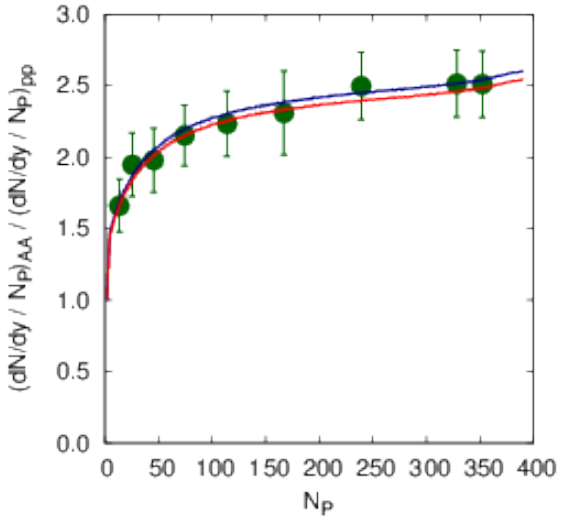

Figure 5. Suppression of ϕ meson production with centrality for Au-Au collision. The red curve is the fit based on the core-corona model [34].

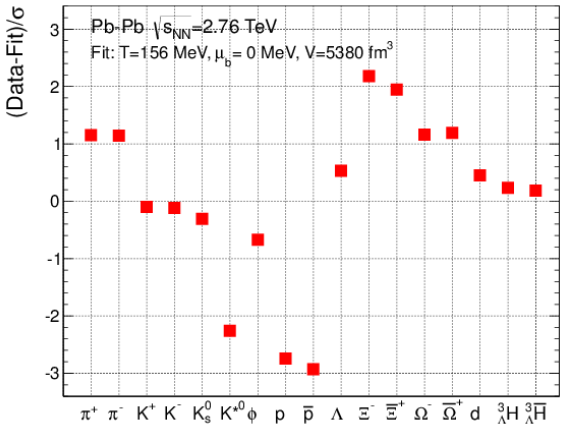

Figure 6. SHM fit to LHC data. Difference (data-fit) in standard deviation units, from Ref. [26].

- Why is there (almost) no strangeness suppression in nuclear collisions?
- Why is the proton/pion ratio at LHC in disagreement with the SHM fit?
- Is the freeze-out curve consistent with the lattice deconfinement critical line?

and, at a more fundamental level,

- Why do elementary high energy collisions show a statistical behavior?

- Why is there a universal hadronization temperature for all high energy collisions?
- Why does hadron freeze-out correspond to $s/T^3 \simeq 7$ or $< E > / < N > \simeq 1.08$ GeV?

In the next sections we shall discuss some possible answers and the separation of the questions in two different groups will become more clear.

4. Statistical hadronization: conservative answers to open questions

Let us now consider the first set of questions for which some answers can be obtained within the SHM or consistently with it.

4.1. Canonical suppression, strangeness enhancement and the ϕ meson

The average particle number in the grand canonical ensemble is given by Eq. (1), which by using the Boltzmann approximation can be written as

$$\langle n_i \rangle^{\rm primary} = \frac{d_i V T m_i^2}{2\pi^2} \gamma_s^{s_i} {\rm K}_2\left(\frac{m_j}{T}\right) \tag{2}$$

where $K_2(x)$ is the Hankel function ($K(x) \sim \exp\{-x\}$ for large x). Notice that the ratio of particle yields is V independent, however, as we shall clarify later, the nature of V in elementary collisions is quite different from that in nuclear collisions and this can effectively lead to different behavior in the two cases.

The local conservation of charges, and in particular of strangeness, has been proposed for quite some time as the mechanism responsible for strangeness suppression [8, 9, 2]. The local strangeness suppression is based on two features. First, one imposes exact strangeness conservation, which leads to a volume-dependent strangeness reduction. However, in elementary collisions with the corresponding overall equivalent cluster volume, the resulting reduction is not sufficient to account for the observed strange particle rates. Hence it was argued that if in a given collision only one pair of strange hadrons is produced, these should appear close to each other spatially, the more so if the medium is relatively short-lived. This approach thus introduces somewhat *ad hoc* a strangeness correlation volume $V_c < V$, within which strangeness has to be conserved exactly. The corresponding model thus now has T, V and V_c as the parameters to be specified by the data, and fits based on such a model provide as good an account for the data as the earlier γ_s scheme [28, 29], with the exception of the ϕ, to which we return later. In Fig. 7 is shown the effect of the strangeness correlation radius, R_c, in the particle yields and the comparison with the grand canonical results. For $R_c \geq 2-3$ fm the canonical suppression almost disappears. In Fig. 8 the values of R_c to fit the data at SPS and RHIC energies is given and extrapolated at LHC energy [30].

A priori little is known about V_c, and in particular, what happens to it in nuclear collisions. The physical origin of V_c has been clarified in Ref. [31] and is due to the causality constraint in the hadronization mechanism.

The evolution of elementary high energy collisions is generally described in terms of an inside-outside cascade [32]. It specifies a boost-invariant proper time τ_q, at which local volume elements experience the transition from an initial state of frozen virtual partons ("color glass") to the almost on-shell partons which will eventually form hadrons. This partonisation time can be estimated most easily in e^+e^- annihilation where the initial quark-antiquark pair is bound by a string of tension σ. When the separation distance R of the initial pair exceeds the energy $2\omega_q$ of an additional $\bar{q}q$ pair, the string breaks and the virtual pair is brought on-shell. For quarks of mass m_q, this energy is determined by $\sigma R = 2\sqrt{m_q^2 + k_T^2}$, where k_T is the transverse momentum of each quark in the newly formed pair. Through lattice simulation [33] $k_T = \sqrt{\pi\sigma/2}$, leading to $R \simeq \sqrt{2\pi/\sigma} \simeq 1$ fm, using $\sigma \simeq 0.2$ GeV^2 and $m_q \ll \sigma$. From this,

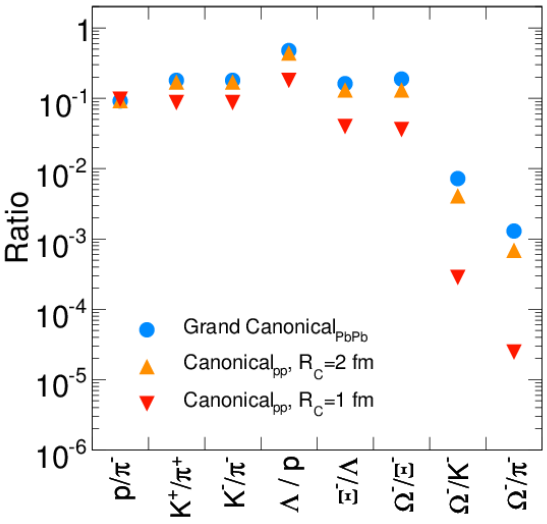

Figure 7. Comparison of grand canonical calculations with the canonical suppression ones, including a correlation volume with radius R_c , from Ref. [30].

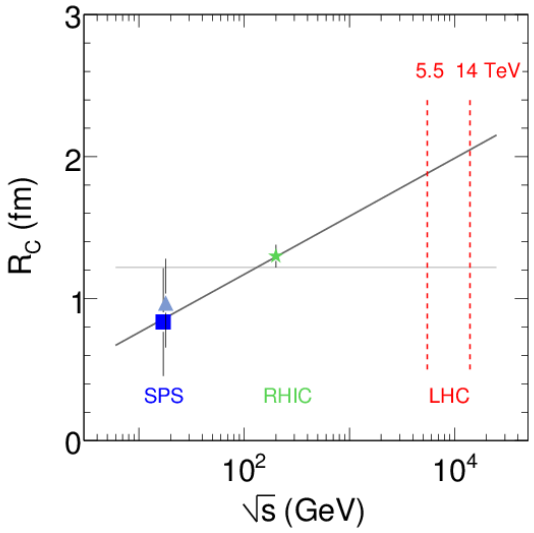

Figure 8. Extrapolation of R_c at LHC energy [30].

we estimate $\tau_q \simeq \sqrt{\sigma/2\pi} \simeq 1$ fm. This process is subsequently iterated, leading to a cascade of emitted $\bar{q}q$ pairs; while the first pair appears at rest in the center of mass of the annihilation process, the subsequent pairs are produced at increasing rapidities. The different pairs will eventually bind to form free-streaming hadrons; for a boost-invariant evolution, this defines a second time threshold, the hadronization time $\tau_h > \tau_q$. The generalization to pp collisions is straightforward: again there is a finite time τ_q needed to bring the partons on-shell, and after a larger time τ_h, these combine to form hadrons. We denote the bubbles of medium for proper time τ, with $\tau_q < \tau < \tau_h$, as "fireballs". Hadronization thus occurs through the formation of partonic fireballs in a cascade of increasing rapidities. It turns out from simple calculations and it is clear from Fig. 9 that there are hadronizing clusters with different spatial rapidity η that are causally disconnected. This remains valid also including the spatial extension of the fireball, defined an evaluated in Ref. [31] as depicted in Fig 10.

The strangeness correlation volume V_c should be identified in fact with that one of a causally connected cluster; causal connectivity thus provides the fundamental reason for local strangeness conservation and hence for the strangeness suppression observed in elementary interactions. It is moreover clear that in nucleus-nucleus interactions, the overlapping fireballs produced at fixed rapidity by the different nucleon-nucleon collisions will give rise to a much larger causally connected volume and thus effectively remove the locality constraints. Moreover, if *very* high energy pp interactions lead to multiple jet production, this could eventually lead to a similar effect, with overlapping clusters from the different jet directions. This is indeed experimentally observed and the strangeness suppression decreases by increasing the energy of the pp collision (in the description of the suppression with γ_s , one has $\gamma_s \simeq 0.6$ for $\sqrt{s} = 200$ MeV and $\gamma_s \simeq 0.8$ at $\sqrt{s} = 900$ MeV).

One can show [31] that the size of the causally connected cluster volumes varies with the fireball life-time,τ_h. An obvious question therefore is whether the fits to production data lead to reasonable cluster sizes. It is found [28, 29] that good fits to data at $\sqrt{s} = 17.3$ and 200 GeV require a strangeness correlation radius of about 1 fm, while leading to the same

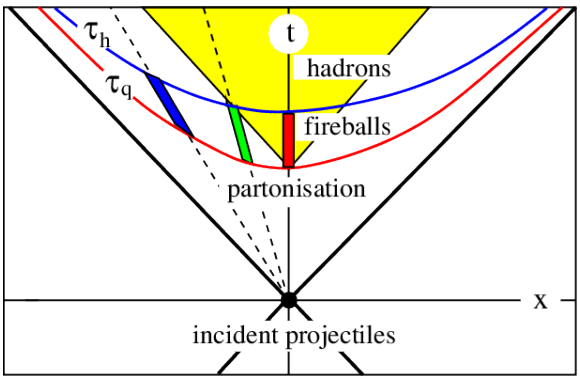

Figure 9. Evolution of the space-time diagram of fireball with no spatial extension. The yellow area indicates the space-time events causally connected with the fireball at rest in the center of mass system.

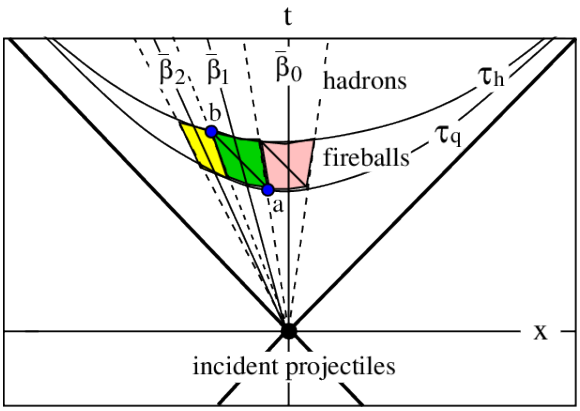

Figure 10. Fireballs with finite spatial extension and their causally connected regions. See Ref. [31] for details.

universal hadronization temperature of about 160 MeV. This is seen [31] to be in accord with a hadronization time τ_h of about 2 - 3 fm. For an evolution of the kind shown in Fig 10 that makes good sense: it takes about 1 fm to form the first $\bar{q}q$ pair, and another to have it hadronize. The causality constraints in elementary high energy collisions thus appears to provide the reason for the observed strangeness suppression, thereby justifying the strangeness correlation model.

However, it should be stressed that the canonical suppression is implemented at hadronic level and therefore there is no suppression for hidden strangeness, i.e. the ϕ meson. Indeed, It is found experimentally that the ϕ meson, consisting of an $s\bar{s}$ pair, is also suppressed, although from a hadronic point of view, it is of zero strangeness. Fig. 5 shows the data on the ϕ suppression for peripheral collisions (similar to elementary pp-collisions) with respect to central ones [34]. In the conventional statistical model with a strangeness suppression factor, the power of γ_s is determined by the number of s plus $\bar{s}$ quarks a given hadron contains. Hence the ϕ gets a factor γ_s^2, which leads to rough agreement with the data. In contrast, in a canonical formulation on a hadronic level, the ϕ does not present any quantum number to be conserved exactly and is not subject to any suppression.

The disagreement of the ϕ abundance may be a signal that strangeness correlation really occurs already on a pre-hadronic level. Requiring exact strangeness conservation for the quark system in the fireball prior to hadronization would in fact result in canonical strangeness suppression of both open and hidden strangeness. A more conservative answer is the core-corona model [34, 35], which is a minimal modification of the SHM and describe the heavy ion scattering as a superposition of a fully equilibrated core (where $\gamma_s = 1$) and single nucleon-nucleon collisions ($\gamma_s < 1$). The corona is indeed defined by the number of nucleons colliding only once , evaluated by Glauber Monte Carlo method. The model introduces a new parameter, essentially describing the non geometrical aspects of the collisions, which is fixed by data in one centrality bin. The red curve in Fig. 5 is the core-corona fit to the ϕ production and the model is successfully applied to many other particle species.

4.2. The proton/pion puzzle at LHC

The unsatisfactory SHM fit to proton production at LHC energy, reported in Fig. 6, is a surprising result since the SHM works very well for nucleus-nucleus scattering up to RHIC energy for particle multiplicities which differ of many orders of magnitude.

Whithin the SHM a solution could be a modification of the resonance spectrum, crucial ingredient in the calculation of the yields, due to low mass resonances (still undetected but predicted by lattice QCD) or to high mass Hagedorn states (HS), with mass m and spectrum $\rho(m) \simeq exp(m/T)$ (see Ref. [36] for a review of the Hagedorn states). At a temperature about 160 MeV, one can populate the hadrons using multihadronic decay reactions, $n\pi \rightarrow HS \rightarrow n^{'}\pi + \bar{X}X$ where $\bar{X}X = \bar{p}p, \bar{K}K, \bar{\Lambda}\Lambda$ and the results are reported in Fig. 11 [37] where the solid black dots represent the situation where there are no initial protons, kaons, and lambdas in the system (while the pions and Hagedorn states begin in chemical equilibrium) whereas the outlined circles represent the scenario when all hadrons begin in chemical equilibrium,

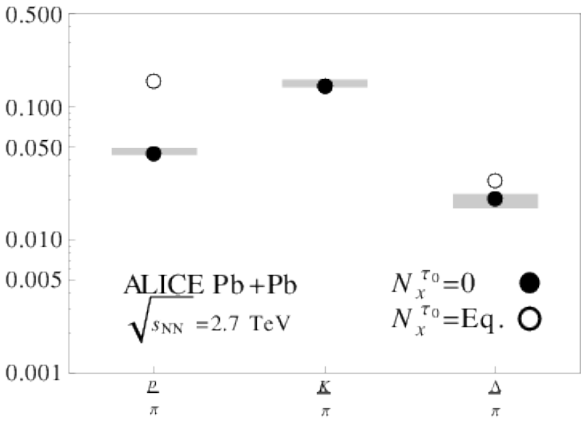

Figure 11. Calculations vs. experimental data points of ALICE at Pb+Pb at $\sqrt{s_{NN}} = 2.76$ TeV from Ref. [37].

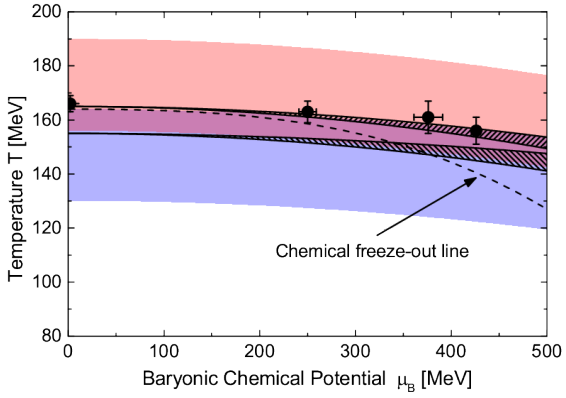

Figure 12. Phase diagram of strongly interacting matter: the coloured areas represent the widths of the crossover transitions. The dashed line is the chemical freeze-out line whilst the reconstructed original chemical equilibrium points in this work are shown as closed circles, see ref.[38].

While the previous proposal depends on a somehow arbitrary modification of the spectrum and a different understanding of the proton/pion puzzle could be the effect of the inelastic reactions between hadrons in the final state which induce changes in the baryon yields and in the chemical freeze-out curve. More precisely, all previous determinations of the points in the (T, μ_B) plane, in the framework of SHM, have implicitly assumed that the primordial hadro-chemical equilibrium (an intrinsic feature of the hadronization process as observed in elementary collisions) remains frozen-in throughout the final expansion phase in heavy ion collisions. On the other hand, the baryon-antibaryon annihilation and regeneration processes do not fall away with the onset of expansive cooling (Ref. [38] and references therein). Their final effect consists of a distortion of the initial, post-hadronization equilibrium yield distribution, in the antibaryon and baryon sector. The dynamical implemenation of this inelastic collisions in the final hadron/resonance expansion phase requires a specific code and the UrQMD hybrid model has been used in Ref. [38, 39]. The differences between the initial and the final hadronic multiplicities after the rescattering stage resemble the pattern of data deviation from the statistical equilibrium calculations, that is the "afterburner" corrections considerably reduces the χ^2 per d.o.f. in Fig. 6 and the freeze-out temperature [38, 39].

The previous "correction" to the standard SHM seems to help to solve another problem. The freeze-out curve converges towards the lattice QCD phase critical line, at small μ_B, but it appears to fall well below the line toward higher values of μ_B. By taking these corrections

into account in the statistical model analysis of the data, one is able to reconstruct the original hadrochemical equilibrium points in the (T, μ_B) plane [38] which closely follow the parton-hadron phase boundary recently predicted by lattice QCD at finite density.

However, the UrQMD hybrid model does not take into account the baryon and antibaryon regeneration. In Ref. [40] it has been clarified that the regeneration process reduces the "afterburner" correction of about $10 - 20\%$ and moreover one has to understand if the same mechanism is at work for hyperons since the resulting suppression is not observed in LHC data.

In conclusions, within the SHM or by introducing some modifications , not in contradiction with the statistical approach, one can answer the first set of questions of Sec. 3. However, the other questions (universal freeze-out temperature at high energy; success of the SHM in elementary collisions; freeze-out criteria) require a more detailed analysis of the dynamics underlying the hadronization process. The recent proposal of considering the hadron production as the Hawking-Unruh in QCD [41, 42] is recalled in the next section.

5. Confinement, string breaking and freeze-out criteria

In high energy heavy ion collisions multiple parton scattering could lead to kinetic thermalization, but e^+e^- or elementary hadron interactions do not readily allow such a description. Moreover, the universality of the observed temperature suggests a common behavior in all high energy collisions or, in other terms, another non-kinetic mechanism providing a common origin of the statistical features.

Indeed a similar mechanism is well known in general relativity: for a black-hole the Hawking radiation [43] has a thermal spectrum (with the limits discussed in Ref. [44]), with the Hawking temperature $T_{haw} = k/2\pi = 1/8\pi GM$, where k is the surface gravity (roughly, the acceleration at the event horizon) and G is the Newton constant. As shown in Ref. [45, 46] this result can be understood in terms of tunneling through the event horizon.

More generally, Unruh [47] discovered that for an observer in uniform acceleration a the Minkowski vacuum corresponds to a thermal bath with a temperature $T_u = a/2\pi$. For the uniformly accelerated observer (Rindler observer) there is an event horizon and the analogue of the Hawking radiation can be evaluated by particle tunneling through the event horizon [48]. It has a thermal spectrum with temperature T_u [47, 49, 41, 48].

It is rather interesting to see if some of the previous considerations apply to QCD dynamics. Indeed lattice simulations and phenomenological analyses indicate that the large distances behavior of the potential V between two static color charges increases linearly with the separation r, $V = \sigma r$. Therefore, QCD at large distances has a typical Rindler force, i.e. a constant acceleration, usually associated with a flux tube (a string) between a quark and an antiquark.

The phenomenological consequences of a constant acceleration and of the breaking of the flux tube in the high energy hadronization process have been analyzed in Ref. [41, 12, 50] with the conclusion that: 1) there is a universal Unruh temperature associated with the hadronization, $T_h \simeq 160 \pm 10$ MeV for massless quarks; 2) a small difference in the acceleration due to quark masses ($m_s \neq m_u = m_d$) explains the strangeness suppression in elementary collisions; 3) this suppression is almost removed in heavy ion collisions.

In this framework a possible understanding [51] of the unexplained freeze-out condition $\langle E \rangle / \langle N \rangle \simeq 1.09$ GeV , for $\mu_B \simeq 0$, seems rather natural. Indeed, the fundamental mechanism of hadronization is quark acceleration or deceleration, leading to string breaking with the resulting pair production and to the universal Unruh temperature. The maximum $\bar{q}q$ separation distance R, previously evaluated for $m_q = 0$, is given by $R = \sqrt{2\pi/\sigma}$.

The Unruh phenomenon, in high energy collisions, is responsible for the production of *newly formed* hadrons, therefore, it cannot address the role of the nucleons *already present* in the initial state of heavy ion collisions. As such, it captures the whole of the freeze-out process only as long as there are no significant baryon-density effects, i.e., only for $\mu_B \simeq 0$, corresponding to

high energy collisions where the large part of produced hadrons are $q\bar{q}$ mesons. Therefore, the energy of the pair produced by string breaking, i.e. of the newly formed hadron is from previous equation, $E_h = \sigma R = \sqrt{2\pi\sigma}$.

In the central rapidity region of high energy collisions, one has $\mu_B \simeq 0$ so that E_h is in fact the average energy $< E >$ per hadron, with an average number $< N >$ of newly produced hadrons. Hence one obtains

$$\frac{< E >}{< N >} = \sqrt{2\pi\sigma} = 1.09 \pm 0.08\ GeV \tag{3}$$

for $\sigma = 0.19 \pm 0.03$ GeV^2.

The possible explanation of the other freeze-out condition, $s/T_{ch}^3 \simeq 7$, is much more subtle. Indeed, in the hadronization process one deals with quantum particles, relativistically accelerated by the strong Rindler force, which experience a spacetime with an event horizon. From this point of view, since there is no gravitational interaction, the corresponding entropy has to be considered as an entanglement entropy due to causally disconnected regions. On the other hand, a quantum field near an event horizon has modes belonging to both sides, inside and outside the horizon, whose entanglement entropy can be computed to give $S_{ent} = \alpha A/r^2$, see, e.g., [52, 53, 54]. Here A is the area of the event horizon, r is the scale of characteristic quantum fluctuations, α is an undetermined numerical constant.

For a black-hole $\alpha = 1/4$ and $r^2 = G$ (in natural units). However, the metric of a uniformly accelerated observer corresponds to the near horizon approximation of a black-hole metric if the acceleration a is equal to the surface gravity k and therefore, by taking the phenomenological point of view of the analogy with the corresponding gravitational horizon, in Ref. [51] $\alpha = 1/4$ has been chosen. The scale of the characteristic quantum fluctuations for the quark-antiquark string is given by $r_T = 1/k_T$.

If for the entropy associated with hadron production at the string breaking the formula

$$S_h = \frac{1}{4}\ \frac{A_h}{r_T^2} = \frac{1}{4}\ \frac{4\pi R^2}{r_T^2} \tag{4}$$

is used with $R = \sqrt{2\pi/\sigma}$ and $T \simeq \sqrt{\sigma/2\pi}$ [41], one gets $S_h = \pi^3$. The entropy *density* divided by T_h^3 at freeze out (for $\mu_B \simeq 0$) turns out to be

$$\frac{s}{T_h^3} = \frac{S_h}{(4\pi/3)R^3T_h^3} = \frac{3\pi^2}{4} \simeq 7.4. \tag{5}$$

compatible with the phenomenological value.

6. Comments and Conclusions

We have seen that all abundances in high energy collisions, including those of strange hadrons, are indeed given by an ideal resonance gas with some improvements/modifications compatible with a statistical approach. The underlying hadronization mechanism of the string breaking can answer some aspects of the comparison of the SHM with data.

We thus find that high energy heavy ion collisions produce essentially a medium which can be considered as hadronic matter in equilibrium, formed at the pseudocritical hadronization temperature predicted by lattice QCD.

However, we want to find in the collision data some sign of the QCD transition, of something like a critical behavior ([55] and reference therein). For example, sufficiently close to a continuous transition, correlations appear at all scales because the correlation length diverges, and in QCD this must produce strong deviations from the ideal hadron gas behavior.

An interesting ansatz to understand hadronization and freeze-out parameter is provided in Refs. [56, 57] which reverse the mechanism of Mott dissociation of hadrons, occuring under compression and heating of hadronic matter as a delocalization of bound states of quarks, and picture the chemical freeze-out as a localization of the quark wave functions in the expanding and cooling fireball. This leads to a description of the chemical freeze-out line in the (T, μ_B) plane.

The study the fluctuations of conserved quantum numbers in an ideal hadron gas, compared to both lattice results and heavy ion data, has been proposed as an signature of the critical behavior (see, for example, Ref. [58]). However, the difference between the HRG and lattice simulations is effectively visible only for quantities which involve high derivatives of P/T^4 with respect to the chemical potentials (i.e. higher cumulants [58, 59]), and therefore the experimental detection requires a large number of events or physical conditions which enhance the fluctuations. Therefore, since a first order phase transition is expected at large μ_B, the future accelerators for heavy ion collisions will have the chance to detect the deconfinement transition by analyzing the strong fluctuations of the conserved charges.

References

[1] J. Cleymans et al., Phys. Lett. **B 242**, 111 (1990); J. Cleymans and H. Satz, Z. Phys. **C57**, 135 (1993); K. Redlich et al., Nucl. Phys. **A566**, 391 (1994); P. Braun-Munzinger et al., Phys. Lett. **B344**, 43 (1995); F. Becattini, M. Gazdzicki and J. Sollfrank, Eur. Phys. J. C **5**, 143 (1998); F. Becattini et al., Phys. Rev. C **64**, 024901 (2001);
[2] P. Braun-Munzinger, K. Redlich and J. Stachel, in *Quark-Gluon Plasma 3*, R. C. Hwa and X.-N Wang (Eds.), World Scientific, Singapore 2004.
[3] F. Becattini, *Universality of thermal hadron production in pp, $p\bar{p}$ and e^+e^- collisions*, in *Universality features in multihadron production and the leading effect*, Singapore, World Scientific (1996), p. 74-104 [arXiv:hep-ph/9701275].
[4] F. Becattini, Z. Phys. **C69**, 485 (1996).
[5] F. Becattini and G. Passaleva, Eur. Phys. J. C**23**, 551 (2002).
[6] S. Borsanyi et al., Phys. Lett. **B370**, 99 (2014).
[7] A. Bazavov (HotQCD collaboration) Phys. Rev. D **90**, 094503 (2014). for a recent review see H-T. Ding, F. Karsch and S. Mukherjee, Thermodynamics of strong-interaction matter from Lattice QCD, arXiv:1504.05274.
[8] R. Hagedorn and K. Redlich, Z. Phys. C27, 541 (1985).
[9] S. Hamieh. K. Redlich, A. Tounsi, Phys. Lett. **B486**, 61 (2000).
[10] K. A. Olive et al. (Particle Data Group), Chin. Phys. **C38**, 090001 (2014).
[11] F. Becattini, P. Castorina, A. Milov and H. Satz, Eur. Phys. J. C **66** 377 (2010).
[12] F. Becattini, P. Castorina, J. Manninen, H. Satz, Eur. Phys. J. C **56** 493 (2008).
[13] A. Andronic, F. Beutler, P. Braun-Munzinger, K. Redlich and J. Stachel, Phys. Lett. **B675**, 312 (2009).
[14] K. Redlich, A. Andronic, F. Beutler, P. Braun-Munzinger and J. Stachel, J. Phys. G **36**, 064021 (2009).
[15] F. Becattini, J. Manninen, M. Gazdzicki, Phys. Rev. C **73**, 044905 (2006).
[16] J. Rafelski and B. Müller, Phys. Rev. Lett. **48**, 1066 (1982) [Erratum-ibid. 56 (1986) 2334]; for a recent review see J. Rafelski and M. Petran, Acta Phys. Polon. Supp. **7**, 35 (2014).
[17] M. Floris, Nucl. Phys. **A931**, 103 (2014).
[18] J. Cleymans and K. Redlich, Phys. Rev. Lett. **81**, 5284 (1998).
[19] J. Cleymans and K. Redlich, Phys. Rev. C **60**, 054908 (1999).
[20] J. Cleymans et al., arXiv:hep-ph/0511094.
[21] P. Braun-Munzinger and J. Stachel, J. Phys. G **28** , 1991 (2002).
[22] V. Magas and H. Satz, Eur. Phys. J. C **32**, 115 (2003).
[23] J. Cleymans et al., Phys. Lett. **B615**, 50 (2005).
[24] A. Tawfik, J. Phys. G **31**, S1105 (2005); Nucl. Phys. **A764**, 387 (2006).
[25] A. Bazazov et al. (HotQCD Collaboration), arXiv:1407.6387.
[26] J. Stachel, A. Andronic, P. Braun-Munzinger and K. Redlich, J. Phys. Conf. Ser. **509**, 012019 (2014).
[27] F. Becattini, P. Castorina, A. Milov and H. Satz, J. Phys. G **38**, 025002 (2011).
[28] I. Kraus et al., Phys. Rev. C **76**, 064903 (2007).
[29] I. Kraus et al., Phys. Rev. C **79**, 014901 (2009).
[30] I. Kraus, J. Cleymans, H. Oeschler and K. Redlich, J. Phys. G **37**, 094021 (2010).

[31] P.Castorina and H.Satz, Int. J. Mod. Phys. **E23** 4, 1450019 (2014).
[32] J. D. Bjorken, Lecture Notes in Physics (Springer) 56, 93 (1976).
[33] M. Luscher, G. Münster and P. Weisz, Nucl. Phys. **B180**, 1 (1981).
[34] F.Becattini and J.Manninen Phys. Lett. **B673**, 19 (2009).
[35] J. Aichelin and K. Werner, Phys. Rev. C **79**, 064907 (2009).
[36] K. Redlich and H. Satz, The Legacy of Rolf Hagedorn: Statistical Bootstrap and Ultimate Temperature, arxiv: 1501.07523.
[37] J. Noronha-Hostler and C. Greiner, Nucl. Phys. **A931**, 1108 (2014).
[38] R. Stock et al., PoS **CPOD 2013**, 011 (2013).
[39] J. Steinheimer, J. Aichelin and M. Bleicher, Phys. Rev. Lett. **110**, 042501 (2013).
[40] Yinghua Pan and S. Pratt, Phys. Rev. C **89**, 044911 (2014).
[41] P. Castorina, D. Kharzeev and H. Satz, Eur. Phys. J. C**52**, 187 (2007).
[42] D. Kharzeev and K. Tuchin, Nucl. Phys. **A753**, 316 (2005)
[43] S. W. Hawking, Comm. Math. Phys. **43**, 199 (1975).
[44] M. Visser , "Thermality of the Hawking flux", arXiv. 1409.7754.
[45] M.K. Parikh and F. Wilczek, Phys. Rev. Lett. **85**, 5042 (2000).
[46] M.K. Parikh, Gen. Rel. Grav. **36**, 2419 (2004).
[47] W. G. Unruh, Phys. Rev. **D14**, 870 (1976).
[48] See for example, A. de Gill, D. Singleton, V. Akhmedova and T. Pilling, Am.J.Phys. **78**, 685 (2010).
[49] W. G. Unruh and N. Weiss, Phys. Rev. **D29**, 165 (1984).
[50] P. Castorina and H.Satz, Adv. High Energy Phys. **2014**, 376982 (2014).
[51] P. Castorina, A. Iorio and H. Satz, Int. J. Mod. Phys. **E24**, 1550056 (2015).
[52] M. Srenidcky, Phys. Rev. Lett. **71**, 666 (1993).
[53] H. Terashima, Phys. Rev. D **61**, 104016 (2000).
[54] A. Iorio, G. Lambiase, G. Vitiello, Ann. Phys. **309**, 151 (2004).
[55] H. Satz, Int. J. Mod. Phys. **A28**, 1330043 (2013).
[56] D. B. Blaschke, J. Berdermann, J. Cleymans and K. Redlich, Phys. Part. Nucl. Lett. **8**, 811 (2011).
[57] D. Blaschke, J. Berdermann, J. Cleymans and K. Redlich, Few Body Syst. **53**, 99 (2012).
[58] See for example, F. Karsch and K. Redlich, Phys. Lett. **B695**, 136 (2011).
[59] C. Schmidt, Nucl. Phys. **A904-905**, 865c (2013).